# Optical switching waves in III-V semiconductor microresonators

I. Ganne, G. Slekys, I. Sagnes, and R. Kuszelewicz
*Laboratoire Concepts et Dispositifs pour la Photonique, Unité Recherche Assoué 250, CNET/CNRS, Boîte Postale 107, 92225 Bagneux Cedex, France*

(Received 1 September 2000; published 1 February 2001)

Experimental evidence of optical switching waves in bistable semiconductor microresonators with fast electronic nonlinearity is presented. Depending on the level of the Gaussian excitation beam, both outward and inward propagating waves are observed. We discuss how their spatiotemporal dynamics influences the range of bistability.

DOI: 10.1103/PhysRevB.63.075318 PACS number(s): 42.65.Sf, 42.65.Pc, 42.65.Tg, 68.65.−k

Transverse effects in optically bistable nonlinear semiconductor microresonators are of practical as well as of fundamental importance. On one hand, such resonators raise considerable interest due to their potential application in all-optical information processing[1] because they offer features of low power, high operation speed, and small size devices.[2–4] Then transverse effects play an important role in the performance of individual discrete bistable devices and, due to cross-talk effects, can seriously limit their packing density. On the other hand, large Fresnel number resonators allow the interaction of a rich variety of physical mechanisms leading to spontaneous and global transverse pattern formation. To a more general extent, self-organized structures suggest new concepts for all-optical information processing.[5]

Transverse aspects of optical bistability appear as soon as one has to account for mechanisms such as diffraction and carrier diffusion.[6] One of the most characteristic effects was shown in spatially extended bistable systems where, under a switching process, a spatial front is formed that displays a smooth transition between two spatial domains of different homogeneous bistable states. Such a switching front (also known as ''kink'' solution) is stable, showing that different spatially separated states can coexist. At the same time switching phenomena naturally involve spatiotemporal dynamics, when a switching front propagates, resulting in the so-called switching wave (SW).[7] Switching waves occur due to carrier transverse diffusion and propagate with a constant velocity depending on the excitation level with respect to a certain value $I_0$, called the Maxwell value of the plane wave hysteresis. As a consequence of the coexistence of two states, this value is defined as the one that evenly splits the area of the hysteresis loop. In this respect the problem is formally identical to phase coexistence in thermodynamics. At $I_0$ exactly, the SW is at rest and establishes equilibrium between the two different states.[6,7] For incident intensities departing from $I_0$, the propagation direction of a SW depends on the sign of this departure. For a Gaussian incident beam, the response of a nonlinear resonator varies in the transverse plane depending on the local incident intensity. Transverse aspects of optical bistability in these conditions were numerically analyzed and radial variations of bistable loops, spatial hysteresis, and changes of the beam profile during bistability switching were discussed.[8,9] So far, switching waves were experimentally observed only in a Fabry-Perot étalon filled with a medium with thermal nonlinearity.[10,11] The phenomenon of a switching wave is of importance for applied research in particular for the minimization of the size of a bistable pixel, but can be interesting as well for transportation of optical information signals. There is also a fundamental interest in the dynamics of switching due to the concept introduced by Rosanov and Khodova[12] that, in a diffracting regime, switching waves may lock together forming stationary localized structures called autosolitons. Localized structures have also been predicted in Kerr-type semiconductor resonators due to the onset of Turing instability in the homogeneous response.[13,14] Such structures can be locally created in the cross section and manipulated in the resonator plane by phase gradients of the holding beams.[15] In the case of a semiconductor microresonator, the transverse spatiotemporal switching dynamics is ruled by carrier diffusion and the role of diffraction is expected to be strongly reduced. It is therefore one of the interest of the study of switching waves to give access to an eventual modification of their dynamics. This modification could originate from the self-interaction of the diffracting oscillatory edges of a cylindrical switching wave subject to an inward collapse.

In this paper we present experimental results obtained on the spatial dynamics of bistable semiconductor resonators and report on transverse switching waves in a passive resonator hosting a fast, electronic nonlinear medium. Moreover quantitative measurements of SW velocities are presented. They are compared to a model previously developed that yields a very good agreement.

Experiments were performed in a semiconductor resonator composed by two Bragg mirrors ($Ga_{0.9}Al_{0.1}As/AlAs$) and a $\frac{3}{2}\lambda$-thick active layer that includes 18 GaAs wells separated by $Ga_{0.7}Al_{0.3}As$ barriers (both 10 nm thick) yielding a gap wavelength around 850 nm. Samples of such microresonators were used in the reflection mode and were excited by a tunable Ti:sapphire laser beam that allowed us to adjust the excitation wavelength with respect to the cavity resonance. The cavity length is chosen so that the cavity resonance wavelength, around 870 nm, is in the Urbach's tail of absorption in an almost purely dispersive defocusing nonlinear regime and the finesse is around 500. In this situation, when the wavelength of the incident beam was tuned below the cavity resonance, a hysteresislike input-output characteristic response was observed. To observe spatial effects, a large

 

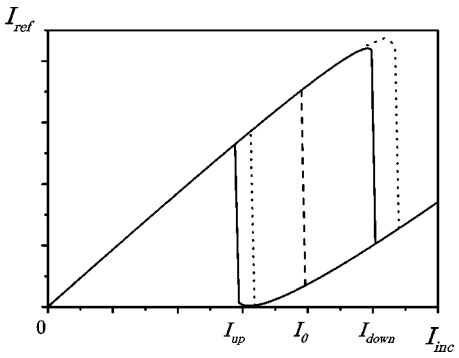


FIG. 1. Schematic picture of a hysteresis cycle in the reflection mode. The solid curve corresponds to the plane wave hysteresis with its respective upper $I_{down}$ and lower $I_{up}$ threshold intensities. The dotted hysteresis results from diffusion and diffraction mechanisms. The vertical dashed line points to the Maxwell intensity $I_0$, located in the middle of the plane wave hysteresis.

aspect ratio is required. Thus, an incident beam of Gaussian profile was focused on the sample with a diameter in the 40–60 $\mu$m range, significantly larger than the diffraction length $a \approx 5$ $\mu$m in our microresonator. To avoid thermal effects, the incident beam was modulated by an acousto-optic modulator generating 4 $\mu$s pulses of rectangular or triangular temporal profile. The near field intensity distribution of the reflected beam was imaged on a charge-coupled device (CCD) camera, which provided time-averaged pictures. Time-resolved images of the near field were taken by a fast intensified CCD camera with a temporal resolution of 5 ns. The temporal signals of the reflected and incident beams were detected with fast Si avalanche photodetectors (Si-APD).

A schematic picture of the hysteresis cycle of the signal reflected from the bistable semiconductor resonator is shown in Fig. 1. The *solid* curve corresponds to the plane wave hysteresis, when diffraction and carrier diffusion effects are absent. When the intensity reaches the switching threshold $I_{down}$ the reflected signal switches down to the low-reflectivity branch of the hysteresis. Then, on the decreasing slope of the incident pulse, when intensity reaches the lower threshold $I_{up}$, the system switches back to the high-reflectivity branch. In the case of limited Gaussian beams the plane wave hysteresis is displaced towards higher intensities due to carrier diffusion and diffraction (dotted hysteresis in Fig. 1). Due also to the effect of switching waves, the lower threshold is increased up to the Maxwell value $I_0$ (dashed curve in Fig. 1), as we discuss below. These contributions are dynamic. Therefore, depending on the time scale a particular mechanism involves, one may need to refer either to the fast (diffusion/diffraction-reduced) or to the static (reduced by switching waves) characteristics. This is why, in the following, we shall refer to the dotted hysteresis as the dynamic hysteresis, ruled by the carrier recombination time scale (1-10 ns range), while the dashed curve will be referred to as the static hysteresis governed by SW propagation (10 ns-1 $\mu$s range).

An experimental hysteresis cycle obtained with the microresonator described above is shown in Fig. 2(b). We used triangular pulses whose duration (4 $\mu$s) was long compared with the dynamic constants of the system, i.e., cavity lifetime ($\sim$10 ps) and carrier recombination time ($\sim$10 ns), and merely corresponds to the static hysteresis as discussed above. It was also possible to polarize the system at arbitrary intensities, using rectangular pulses [Fig. 2(c)].

In the spatial domain, due to the Gaussian profile of the incident beam, the response of the nonlinear resonator is spatially inhomogeneous. Namely, when the maximum of the incident Gaussian beam crosses the switch-down threshold $I_{down}$ [beyond point *A* in Fig. 2(b)], only the central part of the beam switches to the low-reflectivity branch (point *B*) while the periphery of the reflected beam remains in the unswitched state. Time-averaged images of the reflected beam then show spatial equilibrium between the two states of the bistable resonator that establishes after the fast switching dynamics. We note here that even for incident intensities at the

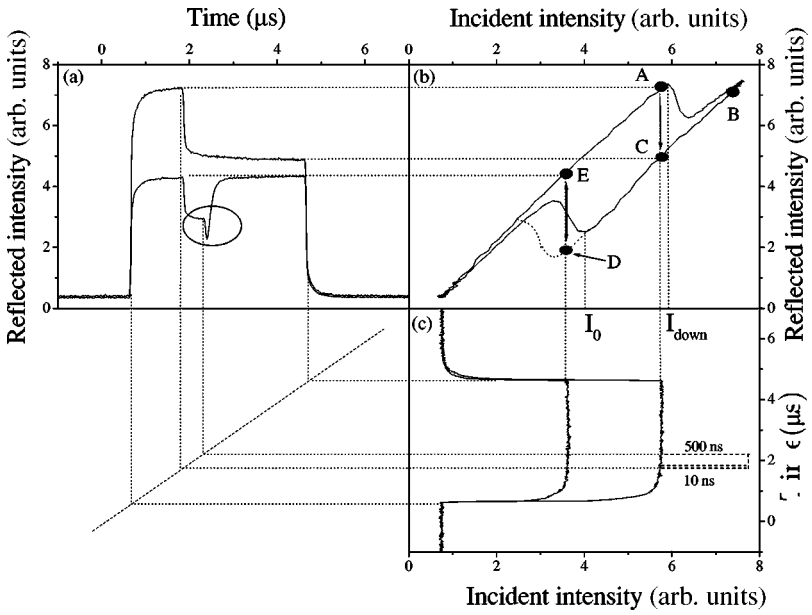


FIG. 2. Temporal traces of (a) reflected and (c) incident pulses. Injection pulses are shown in dashed lines in (c). (b) shows the hysteresis loop obtained in reflection with triangular pulses of 4 $\mu$s duration. The circle in (a) indicates the part of the trace when the lower branch of the dynamic hysteresis is reached and then swept by an inward switching wave. Excitation wavelength: $\lambda = 870$ nm; detuning from cavity resonance: $\delta\lambda = -0.6$ nm.

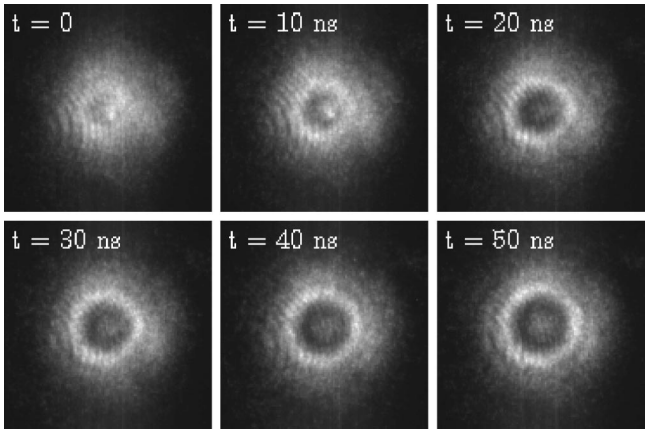


FIG. 3. Fast camera images of an outward switching wave for an incident intensity level slightly below $I_{down}$ threshold. Exposure time of the snapshot images: 10 ns; interval between two images: 10 ns.

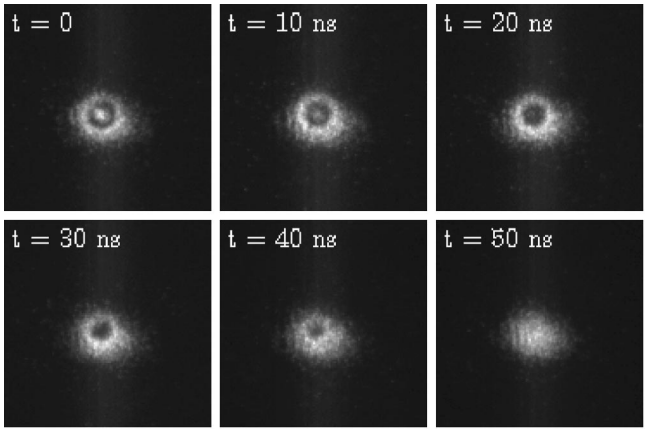


FIG. 4. Fast camera images of an inward switching wave for an incident intensity below Maxwell intensity $I_0$. Exposure time of the snapshot images: 5 ns; interval between two images: 10 ns.

threshold level, the region in the reflected beam concerned by switching has a minimum size that is finite. This gives indirect evidence of the existence of switching waves that we explain in the following way. Threshold is reached at the maximum of the Gaussian incident beam where switch-down occurs first. As the switching intensity is necessarily higher than $I_0$, the switching front that connects two zones at different states starts propagating outwards (outward SW), thus expanding the switched region to the radius at which the intensity equals $I_0$. This results in a dark ring that separates the two domains and corresponds to the isoline of $I_0$ level on the incident beam profile. The diameter of this ring depends on the width of the hysteresis loop and on the incident intensity excess $I-I_0$. Conversely, when decreasing the maximum intensity below $I_0$, the switching front propagates in the other sense generating an inward SW.

To prove the existence of outward and inward SW's and their expected properties, the switching dynamics was investigated using a fast CCD camera and fast Si-APD detectors. For such a purpose in addition to the 60 $\mu$m diameter and 4 $\mu$s duration holding beam, a 5 $\mu$m diameter and short duration (10-500 ns) pulse was superimposed as a temporary injection [dashed lines in Fig. 2(c)], at the center of the holding beam to initiate switching. Temporal signals of reflected and incident pulses were detected by fast detectors and are shown in Fig. 2(a) and 2(c), respectively. At first the holding beam was set slightly below threshold and switching was initiated by a 10 ns injection pulse [upper trace in Figs. 2(a) and 2(c)]. The temporal trace of the reflected signal has two characteristic parts. The first part corresponds to the unswitched state [point *A* in Fig. 2(b)]. In the second part, after the short injection pulse that brings the excitation level above threshold [point *B* in Fig. 2(b)], the system switches down and reflectivity drops to the low-reflectivity branch of the hysteresis loop [point *C* in Fig. 2(b)]. To observe switching waves, a sequence of snapshot images of the reflected beam was recorded during the switching process by the fast CCD camera (Fig. 3). The images were sampled with a 10 ns exposure time and 10 ns lag time between two subsequent images. The injection pulse seen in the first pictures induces an outward SW. The last images show the slowing down of the SW, when it approaches its steady state. To observe inward switching waves, the incident maximum intensity was decreased slightly below the Maxwell intensity level $I_0$ [lower trace in Fig. 2(c)]. In this case, a longer injection pulse (500 ns) was used to avoid transient effects during the switch down process. In this situation, the temporal trace of the reflected signal [lower trace in Fig. 2(a)] has three parts: an unswitched level at the beginning of the holding pulse [point *E* in Fig. 2(b)], a switch-down part under the effect of the injection pulse (from *E* to *D* via *B*), and finally, a switch-up back to the initial state on the high-reflectivity branch (from point *D* to *E*) due to the inward propagation of a SW. Fast camera images taken immediately after the injection pulse, i.e., during the switch-up process are given in Fig. 4. In this case the switching front propagates to the center of the beam and tends to establish stationary equilibrium between two states. But this equilibrium is not reached since the incident peak intensity is smaller than $I_0$ and, finally, the unswitched state prevails over the switched state. As the switched zone collapses, the system returns to the unswitched state [point *E* in Fig. 2(b)], leading to the recovery of the Gaussian profile of the reflected beam (last images in Fig. 4).

Different propagation directions of SW's below and above $I_0$ may have the following physical interpretation. $I_0$ intensity corresponds to the critical intensity level, sufficient to maintain the high excitation domain stable and stationary. At higher excitation levels $I>I_0$, the density of carriers is high enough so that diffusion towards the adjacent low excited domain may stimulate switch-down and generate thereby an outward SW. At lower excitation levels $I<I_0$, carriers also diffuse, but their density is not sufficient enough to induce switching in the adjacent zone. Conversely, by decreasing the carrier density at the internal boundary of switched zone, diffusion stimulates there a switch-up process and generates an inward SW. An important point in the trace of the reflected signal is the significant decrease of the reflected intensity before switch-up [Fig. 2(a)]. At the minimum of the peak, reflectivity is lower than expected from the

hysteresis curve given in Fig. 2(b) because in this case the response follows (via point $D$) the dynamic hysteresis loop which has lower switch-up threshold [see dashed parts of the hysteresis in Figs. 1 and 2(b)]. It is the transient phenomenon that illustrates the effect of SW on the hysteresis width. In this case, when the intensity decrease below $I_0$ is faster than the dynamic response of the system, the lower branch of the dynamic hysteresis can be reached. But then the spatiotemporal dynamics of inward SW takes place and switches up the whole region defined by $I<I_0$. Thus the lower threshold shifts towards $I_0$ and the bistability range is reduced to the static hysteresis. This experiment emphasizes the time-scale dependence of the hysteresis loop.

To measure velocities of SW's, spatially resolved temporal signals were measured with the fast pointlike Si-APD detector. For such a purpose the reflected beam was magnified ($30\times$) and the near field was imaged on the 50 $\mu$m aperture of the detector, which was mounted on a translation stage in order to scan a radius of the cross section of the reflected beam. The temporal signals of the switching fronts were recorded for different radial coordinates of the reflected beam. To reduce the errors pertaining to the finite aperture of the detector, we used the inflection points of the switch-down and switch-up temporal slopes as the switching front arrival time. Two sets of curves, corresponding, respectively, to outward and inward SW's were measured, and the dependence of the arrival time of the switching front upon the radial distance from the beam center was determined. The corresponding plots for inward and outward waves are presented in Fig. 5. To compare experimentally measured velocity values with theoretical predictions we made use of the velocity law[16,17]

$$v(r)=\frac{dr}{dt}\propto I(r)-I_0, \tag{1}$$

which was demonstrated on the basis of the solutions of generalized Fisher equations[19] and whose validity relies on the ability of the system to be described by a third-order equation for the normalized intracavity field[18]

$$\frac{\partial u}{\partial t}-\Delta_r u=C(-u^3+\alpha u+a), \tag{2}$$

where $\Delta_r$ is the radial Laplacian $C$ and $\alpha$ are constants defined by the system parameters and $a$ is the normalized incident intensity proportional to $I-I_0$. Such a system allows solutions propagating with a velovity $v$. In direct gap semiconductors the velocity is expressed by Eq. (1). For the case of Gaussian incident beams Eq. (1) can be reformulated as

$$v(r)=A\left\{I_m\exp-\left[\frac{1}{2}\left(\frac{r}{w}\right)^2\right]-I_0\right\}, \tag{3}$$

where $w$ is the waist of the reflected beam, $I_m$ is the maximum intensity, $I_0$ is the Maxwell intensity, and coefficient $A$ is a fit parameter. $I_0$ was measured experimentally above threshold conditions, and corresponds to the incident intensity at the radius of the dark ring appearing in the spatial profiles of the reflected beam. Using this expression for velocity, the arrival time $\Delta t(r)$ of the switching front at the radial coordinate can be calculated as

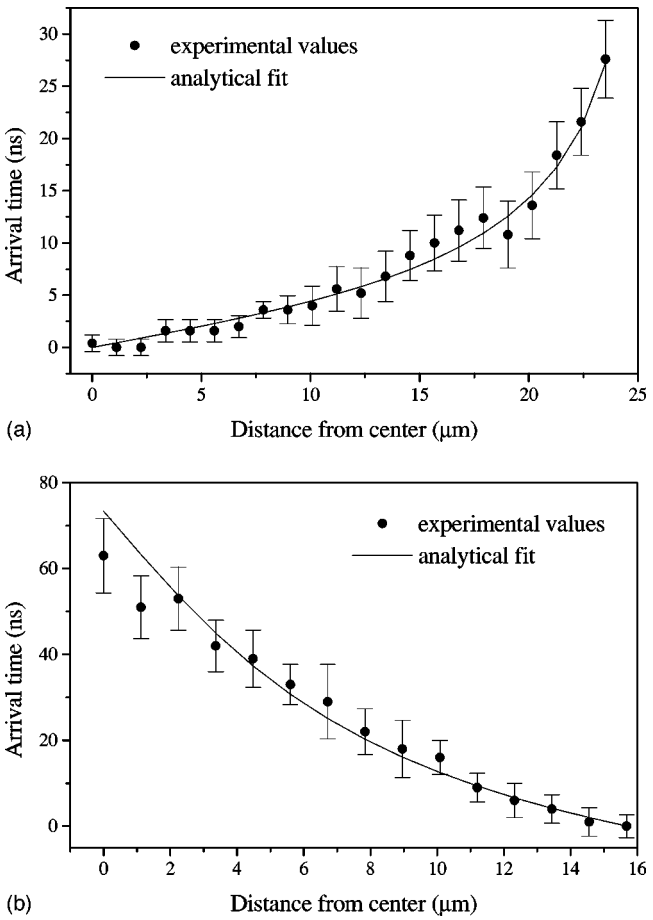


FIG. 5. Arrival time of the switching front versus distance from the center of the reflected beam, for (a) outward and (b) inward switching waves. Circles denote experimental values and straight line corresponds to the analytical fit defined in the body.

$$\Delta t(r)=\int_0^r\frac{dr'}{v(r')}. \tag{4}$$

Figure 5 shows the experimentally measured dependence of the arrival time of outward and inward SW versus radial position, and yields good agreement with their respective analytical fits. The maximum velocity of the outward SW occurs at the center of the beam and is equal to 2.5 $\mu$m/ns, while the velocity of the inward SW is maximum in the periphery of the beam and is equal to 0.6 $\mu$m/ns. The difference between these maximum velocities is explained by the fact that the deviation of the incident intensity from $I_0$ can be significantly larger in the case of outward waves, with respect to the case of inward waves where this deviation is limited by the dynamical increase of the lower threshold. We note the difference in the switch-up process, when the holding intensity is smaller than the lower threshold of the dynamic hysteresis. In the latter case, switching occurs locally through recombination, without involving SW's. We note also that, when reaching the beam center, the inward wave

exhibits a clear departure from the theoretical curve in the form of an accelerated collapse [Fig. 5(b)]. Diffraction would rather delay the process of collapse and cannot therefore be invoked. Conversely, we interpret this acceleration by the failure of the one-dimensional description on which the velocity law relies, when the radius of curvature of the switching wave becomes comparable to the diffusion length. This observation thereby assesses the prevail of diffusion over diffraction in nonlinear semiconductor microresonators.

In conclusion, we have shown experimental evidence of switching waves in bistable semiconductor resonators with a fast electronic nonlinearity. We have also evidenced that spatio-temporal dynamics of switching waves is at the origin of the reduction of the bistability range, by increasing the lower threshold towards Maxwell value of intensity. Depending on the excitation intensity, switching waves with different senses of propagation were excited and observed. Finally, we measured the switching wave velocity dependence upon the excitation excess and found it in very good agreement with theoretical predictions.

This work was supported by ESPRIT LTR Project 28235 PIANOS. The authors thank Professor N.N. Rosanov and Dr. M. Brambilla for enlightening discussions.

[1] H.M. Gibbs *Optical Bistability: Controlling Light with Light* (Academic, New York, 1985).
[2] O. Sahlen, U. Olin, E. Masseboeuf, G. Landgren, and M. Rask, Appl. Phys. Lett. **50**, 1559 (1987).
[3] R. Kuszelewicz, J.-L. Oudar, J.C. Michel, and R. Azoulay, Appl. Phys. Lett. **53**, 2138 (1988).
[4] T. Rivera, F.R. Ladan, A. Izraël, R. Azoulay, R. Kuszelewicz, and J.L. Oudar, Appl. Phys. Lett. **64**, 869 (1994).
[5] L. Lugiato, M. Brambilla, and A. Gatti, *Optical Pattern Formation*, Vol. 40 of Advances in Atomic, Molecular, and Optical Physics (Academic, Boston, 1998), p. 229.
[6] W.J. Firth, I. Galbraith, and E.M. Wright, J. Opt. Soc. Am. B **2**, 1005 (1985).
[7] N.N. Rosanov, V.E. Semenova, and G.V. Khodova, Kvant. Elektron. (Moscow) **9**, 354 (1982). [Sov. J. Quantum Electron. **12**, 193 (1982)].
[8] J.V. Moloney, M. Sargent, and H.M. Gibbs, Opt. Commun. **44**, 289 (1983).
[9] A.V. Grigor'yants and I.N. Dyuzhikhov, J. Opt. Soc. Am. B **7**, 1303 (1990).
[10] S.P. Apanasevich and A.V. Lyakhnovich, Phys. Status Solidi B **150**, 507 (1988).
[11] A.V. Grigoriants, L.L. Golik, Yu.A. Rzhanov, Yu.I. Balkarei, and M.I. Elinson, Kvant. Elektron. (Moscow) **14**, 1247 (1987) [Sov. J. Quantum Electron. **17**, 793 (1987)].
[12] N.N. Rosanov and G.V. Khodova, Opt. Spektrosk. **65**, 761 (1988) [Opt. Spectrosc. **65**, 449 (1988)].
[13] M. Tlidi, P. Mandel, and R. Lefever, Phys. Rev. Lett. **73**, 640 (1994).
[14] M. Brambilla, L.A. Lugiato, F. Prati, L. Spinelli, and W.J. Firth, Phys. Rev. Lett. **79**, 2042 (1997).
[15] W. Firth and A. Scroggie, Phys. Rev. Lett. **76**, 1623 (1996).
[16] N.N. Rosanov, Opt. Spektrosk. **71**, 816 (1991).
[17] B.G. Sfez, R. Padjen, and J.L. Oudar, Conference QELS'91, Q-TuI-34, Baltimore, 1991.
[18] B.G. Sfez, Ph.D. dissertation, University Paris-Sud Orsay (1991).
[19] P. Kaliappan, Physica D **11D**, 368 (1984).